Recent progress of laser micro- and nano manufacturing

Weiping Zhou[1], Denzel Bridges[2], Ruozhou Li[2], Shi Bai[1], Ying Ma[1], Tingxiu Hou[1], Anming Hu[1, 2 *]

[1]*Institute of Laser Engineering, Beijing University of Technology, 100 Pinle Yuan, Chaoyang District, Beijing 100124, China*

[2]*Department of Mechanical, Aerospace and Biomedical Engineering, University of Tennessee Knoxville, 1512 Middle Drive, Knoxville, TN 37996, USA*

[*] E-mail: anminghu@bjut.edu.cn

Abstract

Micro devices and information technologies have been improved as a result of decreasing the finest manufacturing feature, a lower energy cost and increasing of integration and operating speed. A broad range of microfabrication technologies have been developed for different applications. However, these conventional microfabrication techniques are not suitable for a diversity of nanomaterials and the construction of complicated three-dimensional nanostructures. Laser based micro/nano-manufacturing technologies have emerged in recent years to address relevant issues because of its applicability to virtually all kinds of materials at a small scale down to nanometers. The aim of this paper is to give an overview of various latest laser techniques sorted into four main areas: 1) near field laser fabrication, 2) far field laser interference lithography and laser direct writing for nanofabrication, 3) laser manufacturing of nano materials, 4) stimulated-emission-induced depletion (STED) assisted laser fabrication. The review also covers major progresses achieved by Dr. Anming Hu's group, such as, femtosecond laser-induced nanojoining, laser exfoliation of porous graphene, nanograting fabricated with laser interference lithography, and microlens femtosecond laser fabrication. We further discuss the

challenges in laser based micro and nano manufacturing and present outlooks in the near-term development.

Keywords: micro and nano manufacturing, near field laser fabrication, laser direct writing, stimulated-emission-induced depletion

Contents

1. Introduction

Micro- and nanostructures have a wide range of applications in electrical, mechanical, biological, and optical fields[1]. The need for nano-manufacturing is driven not only by the requirement of increasingly hybrid devices and structures with novel properties but also by the trend of decreasing building block sizes, material usages and energy consumption. To meet the demand for product miniaturization in emergent nanomechanical electrical systems (NEMS), a logical step is to achieve the desired high precision and resolution at a nanoscale through the development and wide implementation of nanofabrication technologies. Traditional fabrication methods for structures at the micro- and nanometer scales use techniques rooted on the semiconductor industry. The standard nanofabrication process involves electron beam

direct writing designed patterns and optical projection lithography using a set of masks at a high throughput level. Also there are several other techniques for the next generation lithographies such as extreme UV lithography, X-ray lithography, electron and focused ion projection lithography.

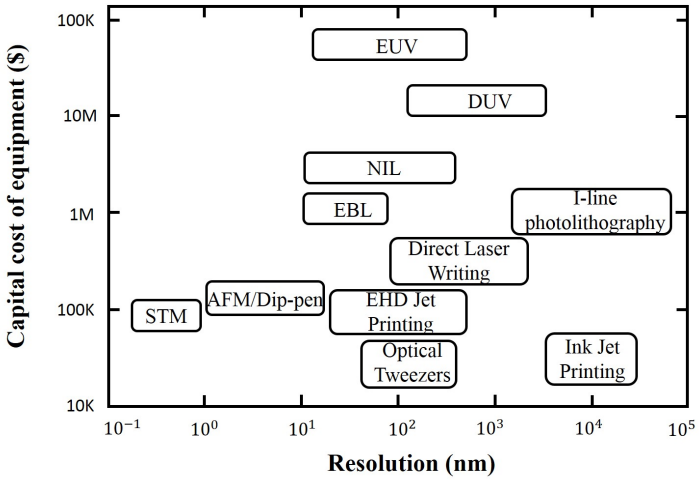

Figure 1 Equipment cost and minimum resolution of micro and nano manufacturing methods. EUV:extreme UV lithography, DUV:deep UV lithography, EBL:electron-beam lithography, NIL: nanoimprint lithography, STM:scanning tunneling microscopy, AFM:atomic force microscopy. Adapted from ref. 2.

The equipment cost and minimum resolution of these micro and nano manufacturing are shown in Figure 1. Most of these methods generally referred to as very expensive top-down-methods, insufficiently flexible for new development. In contrast, laser manufacturing enables a bottom-up process. The high power density in the vicinity of the focus of a pulsed laser (>10^6 W/cm^2) allows this method to be applied to processing almost all materials. Laser materials processing has been successfully applied in cutting, welding, drilling, cleaning, additive manufacturing, surface modification and micro-machining for several decades[3]. In most cases, the feature size and resolution are the primary parameters. The diffraction limit of the laser beams is governed by:

$$d = \frac{\lambda}{2n \sin \alpha}$$

where d is the minimum beam spot diameter, λ the laser wavelength, n the refractive index of the medium of beam delivery to the target material and α the beam divergence angle. According to this formula, the best theoretical resolution of laser processing is around half of the laser wavelength. Considering the optical wavelengths of lasers (within 248 nm-10.6 mm), there are considerable challenges to achieve nano-scale (≤100 nm) resolution in direct laser fabrication.

To improve the fabrication resolution many methods have been used including the use of high numerical aperture optics and shorter wavelength light sources. For a numerical aperture of 0.48 and a wavelength of light source of 365 nm, the processing resolution down to 500 nm has been achieved[4]. For a resolution less than 100 nm, the numerical aperture should be risen up to 0.6, with the used of 157 nm wavelength laser. The option seems practically, however, these improvements are costly. Another disadvantage is that the deep ultra-violet light sources are unstable in light intensity. Also most of the parts of the apparatus need to be in vacuum or dry high purity N_2 gas protection chamber to avoid the strong absorption of the UV radiation. Therefore to overcome these shortcomings, various methods have been developed, such as, near-field process, multiphoton effect, stimulated emission depletion (STED) inspired laser direct writing. We will overview the latest progresses in these fields. The objective of this review aims to provide a comprehensive understanding of the progresses in development of laser based nano-manufacturing technologies and associated sciences to fabricate objects with a size smaller than a micrometer.

The article is organized as follows: Following the first part of introduction, near field laser fabrication is reviewed in the 2nd section. It contains near field interference lithography, scanning near field photolithography using laser coupled near field scanning optical microscopy, nano ridge aperture (bowtie) beam transmission enhanced nanofabrication, particle lens array nanofabrication and solid embedded lens laser writing. The third section talks about far field laser interference lithography and laser direct writing for nanofabrication. The fourth section focuses on laser manufacturing of nano materials. It contains laser manufacture of nanoparticles nanotubes and nanowires, femtosecond laser-induced nanojoining, and laser writing embedded microlens. The fifth section presents stimulated-emission-induced depletion (STED) assisted laser fabrication. The last part is about the summary and outlook.

2. Near field laser fabrication

1) Near field interference lithography

Near-field interference lithography is based on an evanescent (non-propagating) wave or surface plasmon interferences, providing a new route to overcome the diffraction limit. The first demonstration of evanescent interferometric lithography was completed by Blackie using a mercury arc lamp[5,6]. Laser based evanescent wave near field lithography using total internal reflection (TIR, shown in Figure 2) was subsequently reported by Martinez-Anton[7]. A prism was irradiated with split 405 nm wavelength laser beams at an angle to enable the total reflection and create periodic

evanescent waves. Periodic surface relief gratings of around 100 nm period were produced on photoresists using this technique[7].

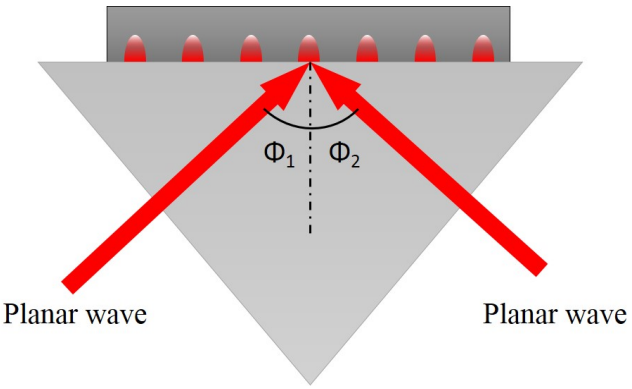

Figure 2 Illustration of a typical TIR optical configuration to generated evanescent waves through interference of tow intersecting beams. Adapted from ref. 7.

Later on, Chua [8] constructed four beams evanescent waves interference lithography, using the interference of multiple counter-propagating evanescent waves to print periodic two dimensional features. Their numerical simulation results suggested that this technique enables fabrication of periodic two dimensional features with resolution less than one third of the irradiation wavelength. The resolution is further significantly promoted to subwavelength by Bezus [9]. In their work, guided-mode resonant gratings are used to generate interference patterns of the evanescent waves. The interference pattern feature size is up to 8 times smaller than the incident wavelength and the intensity at the interference maxima exceeds the incident wave intensity by an order-of-magnitude. Murukeshan investigated the influences of polarization and exposure duration on patterning by evanescent waves interference lithography[10]. Their results suggest that this technique is capable to achieve nanoscale linewidths as small as 15 nm, a pitch size of 105 nm, and an aspect ratio as high as 10.7. The drawbacks of this method are that the depth is shallow due

to the non-propagating nature of the evanescent wave, and the energy transmission through the masks is also very low.

To overcome these drawbacks, surface plasmon interference lithography (SPIL) can be a solution. This SPIL technology is based on field enhancement of surface plasmon waves induced around nanoscale metallic structures and dielectric interface. If the metallic mask is very thin (e.g. 50 nm), surface plasmon waves can be generated on both sides. The enhancement, due to the coupling between the surface plasma waves and the evanescent waves, can be several orders of magnitude in intensity compared to the incoming beam. Meanwhile, the wavelength of the excited surface plasmon wave is shorter than that of the exciting laser at the same frequency. Therefore the excited surface plasmon wave takes the dominant role while higher resolution is expected. Typically, the wavelength of the exciting laser, λ(i,j), needs to match the materials and the structures of the mask. Their relationships can be found as follows[11]:

$$\lambda(i,j) = \frac{a}{\sqrt{i^2 + j^2}} \sqrt{\frac{\varepsilon_d \varepsilon_m}{\varepsilon_d + \varepsilon_m}}$$

where a is the metallic mask periodic nanostructure period, ε_d and ε_m the dielectric constants of the mask metal and the surrounding dielectric medium, respectively and i, j mode indices, separately. A larger period allows longer exciting wavelengths. The SPIL technique for the fabrication of periodic surface nanostructures was first reported in 2004[11],[12] using an aluminum or silver mask. An example of a typical configuration for the SPIL technique is shown in Figure 3.

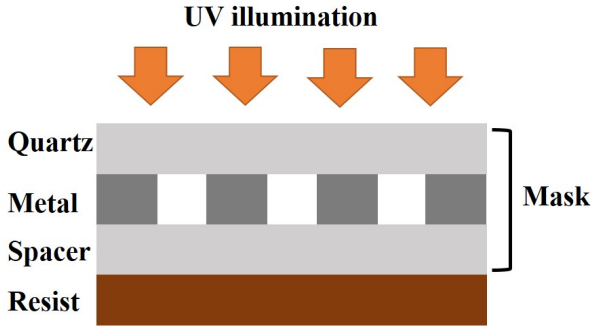

Figure 3 A typical process configuration for SPIL and an optical mask.

Liu[13] proposed the nanophotolithography technique based on the interference of surface plasmon waves. Their simulation results show uniform interference patterns far beyond the free-space diffraction limit of the light. The effect of the ratio lines to spaces for nanolithography using surface plasmons was investigated based on FDTD simulation by Kim[14]. A periodic feature of sub-60 nm which corresponds to a size less than λ/7 can be obtained with a 1 μm period of the mask. Using a specially designed sandwich anisotropic metamaterial structure posited beneath a conventional chromium mask[15], a uniform interference pattern can be obtained with feature size about 40 nm, smaller than 1/11 of illumination wavelength at 442 nm.. Sreekanth compared standard far field laser interference lithography, near field evanescent wave lithography and the SPIL techniques[16]. They found that that the SPIL technique can produce deeper features than the evanescent wave lithography technique.

2) Scanning near field photolithography using laser coupled near field scanning optical microscopy

Scanning near field photolithography (SNP) is based on the coupling of a laser beam with a tapping optical fiber. A very tiny tip of optical fiber (typically 50 nm) in the microscope scanned closely (10-20 nm) to the target surface as shown in Figure 4.

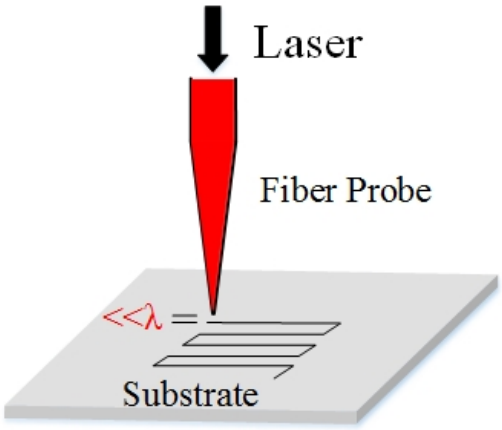

Figure 4 schematic diagram of scanning near field photolithography.

A high resolution evanescent energy field is generated at the tip. The nanometer distance between the tip and target ensures that the evanescent wave arrives at the target surface with sufficient energy density which decays exponentially with increasing the tip-to-surface distance. The patterned photoresist is further post-processing by chemical etching, plasma etching or UV light irradiation to create nano patterns. Kingsley[17] reported an ultracompact near-field optical probe based on a single, integrated assembly consisting of a gallium nitride (GaN) light-emitting diode (LED), a microlens and a cantilever. The cantilever contains a hollow pyramidal probe with a subwavelength aperture at its apex. Using this probe a resolution of 35 nm, corresponding to λ/10, can be obtained. Sun and Legget[18,19] selectively oxidized a strongly bound self-assembled nanolayer (SAM) photoresist on a gold substrate using a SNP technique. A chemical etching process is followed to realize 20-55 nm resolution in surface patterning. This resolution comparable with electron beam lithography but omitted the vacuum chamber. In the coupled laser and NSOM nano-fabrication technique, the probe-to-sample distance is a critical parameter to control both the size and shape of nano-features. With a small probe

diameter and probe-to-substrate distance, the NSOM overcomes the traditional far-field diffraction limit and can be used for sub-wavelength patterns. Dam[20] fabricated nanotip arrays on the distal faces of coherent fiber-optic bundles. The nanotip array comprised ~6000 individual optical fibers that were etched chemically. These tips were ~4 mm long with radii of curvatures as small as 15 nm. Krausch[21] used uncoated glass fiber tips showing that lateral resolution can be well beyond 100 nm in scanning near-field optical microscopy in the internal reflection mode. An aperture-less NSOM is reported by Grigoropoulos[22]. A metallic AFM tip is employing for surface plasmonics excitation. This apertless NSOM successfully written 14 nm width grids in 25 nm gold films. Another key parameter of this method is the fabrication speed. A new lithography technique was proposed by Kuwahara[23] using a super-resolution near-field structure (Super-RENS) for high-density data storage. Narrow grooves with less than 200 nm full-width at half-maximum (FWHM) were obtained. Moreover, the fabrication speed is 10^4 or 10^5 times greater than that with the conventional techniques using a near-field scanning optical microscope. The drawback of SNP is that it requires of high precision nano-distance control between the fibre tip and the target. If the target surface is rough then it is difficult to apply the technique for uniform pattern writing.

3) Nano ridge aperture (bowtie) beam transmission enhanced nanofabrication

The amount of light transmission through a small aperture of an object depends on the aperture size, d_a, and the wavelength, λ, of the light source. If an aperture is smaller than the laser wavelength, the light transmission is restricted. Take a circular

aperture for example, the transmission efficiency can reach to the order of $(d_a/\lambda)^4$ due to the optical diffraction effect[24]. It was found that, with a specific aperture geometry such as a bowtie or H, high energy laser beams can be delivered through the aperture with much less attenuation than a circular aperture. This energy is sufficient to produce nanoscale patterns on a surface through a contact lithography[25,26]. The enhancement was found to be due to the near field surface plasmonic effect[27]. Figure 5 shows a typical structure of a bowtie aperture.

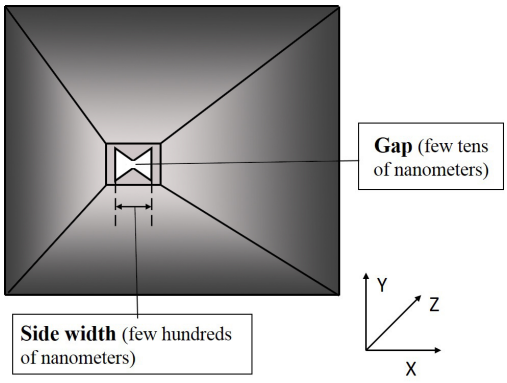

Figure 5 Scholastic structure of a typical nano bowtie aperture

Wang[28] demonstrated bowtie apertures with a 30 nm gap size in aluminum thin films coated on quartz substrates. Holes of sub-50-nm dimensions can be fabricated in photoresist by illuminating the apertures with a 355 nm laser beam polarized in the direction across the gap. Using bowtie apertures with the assistance of the interferometric spatial-phase-imaging (ISPI) technique can also be used for optical parallel nanolithography[29]. The ISPI system can detect and control the distance between the bowtie aperture and photoresist in a sub-nanometer resolution. This conquered the difficulties due to the light divergence of bowtie apertures. A feature size of 22 ± 5 nm can be achieved using parallel nanolithography. However, these previous work is limited to using a single source. One approach made by Uppuluri[30]

describes using a nanoscale bowtie aperture array for parallel nanolithography. In addition to the optical issues related to a nanoscale bowtie aperture, they also reported other manufacturability considerations such as reducing the friction between the metal film and the photoresist surface. Their experiments achieved parallel patterning, with a resolution in the order of 85-90 nm and high repeatability. Nevertheless, fabrication of reproducible structures between scans is still challenging. A recent theoretical study shows that near field enhancement is dramatically influenced by the coating thickness and tip shapes[31]. The variations in the surface topography of the substrate and differences in the shape of the tip are the unsolved issues.

4) Particle lens array nanofabrication and solid embedded lens laser writing

This technique is based on the use of self-assembled mono-layer transparent micro spherical particles. Due to laser light intensity enhancement near the contact area between particles and substrate, high resolution patterning can be realized. Figure 6 shows the schematic diagram of this technique for direct laser writing of nanoline on substrate surface by a scanning process with laser beam. Also this method can be used to fabricate complex patterns[32].

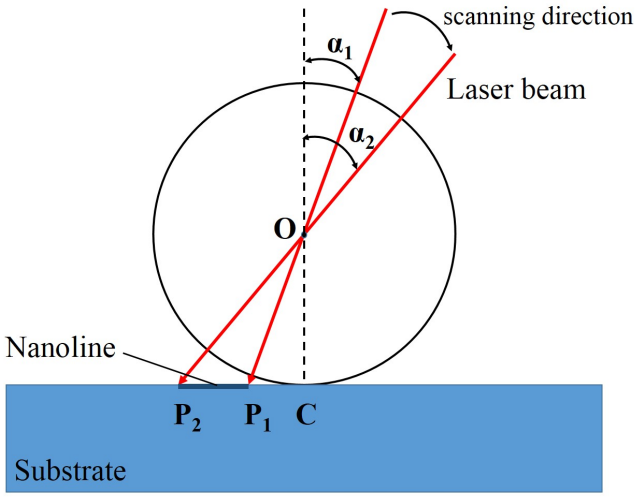

Figure 6 Schematic diagram of the experimental configuration for direct laser writing of nanoline on substrate surface. (α_1, α_2 incident angle of laser beam scanned from different angle, P_1, P_2: intensity peak on substrate for angular beam, c: contacting point, o: coordinate origin). Adapted from ref. 32.

The use of self-organized closed packed monolayer microspheres for laser nano-patterning on large areas was first reported by Hasegawa[33]. They generated 95 nm structures on a polymer surface. Mie theory was applied to calculate the near field intensity (electrical vector) enhancement effect of polystyrene micro-sphere irradiated by an 800 nm wavelength laser beam. They found that the energy field is not focused beyond a distance, d_f, from the sphere in air:

$$d_f = r\frac{2-n}{2(n-1)}$$

where n is the refractive index of the sphere and r is the radius of the sphere. When the microsphere size is shorter than the light wavelength, two focusing peaks were found with double spots generated on substrate surface. For the practical applications of this technique, the microsphere diameter should be normally greater than wavelength. Sakai[34] reported on the dependence of the size parameter in the Mie scattering theory on the nano-processing properties with small polystyrene (PS) particles. In their experiment, 800 nm and 400 nm wavelengths femtosecond laser

pulses were used. With the 800 nm wave, the patterned hole diameter ranged from 100 to 250 nm and the depth ranged from 20 to 100 nm. With the 400-nm wave, the hole diameter ranged from 50 to 200 nm while the depth ranged from 10 to 60 nm. Brodoceanu[35] used a regular lattice of amorphous silica microspheres as a microlens system for laser-induced single-step fabrication on a (100) Si surface. With single-pulse 265.7 nm femtosecond-laser radiation, hole diameters of 57±6.5 nm at full width at half maximum and depths of 6±1 nm can be achieved. However, the enlarged particle size leads to a larger focused energy field spot area, thus reducing fabrication resolution. In order to obtain a smaller light enhancement region, a small particle size needs to be selected with the content of a weaker light enhancement effect[36]. Similar as other particle lens array based techniques, this method shows difficulties to obtain well uniformed due to the variation of beam intensity and the possibility of non-monolayer particles at some locations.

Solid immersion microscopy [37] provides another method to approach sub-wavelength resolution in air. Significantly higher optical throughput can be achieved by focusing light through a high refractive-index solid immersion lens (SIL) held close to a sample. The minimum resolution of a focusing system is inversely proportional to numerical aperture (NA), where NA=n×sinθ, θ is the maximum angle of incidence, and n is the index of refraction at the focal point. Kim[38] achieved a patterning resolution of 70 nm and a speed of 100 mm/s with a 20 nm gap between the plasmonic optical head and substrate. Park[39] proposed the lithography method with high throughput can make an optical spot with a diameter of the order of 10 nm

and can perform nanopatterning at sub-m/s speed. Milster[40] discussed a new maskless lithography concept by employing an array of solid immersion lens (SIL) nano-probes. These nano-probes are efficient near field transducers. Each transducer combines a SIL, a dielectric probe tip and an antenna structure. They demonstrated the feasibility to fabricate an efficient array of near-field transducers. The optical spot dimension is around 20 nm when illuminated by a 405 nm laser diode source.

Different from above, Hoffnagle[41] described deep-ultraviolet interferometric lithography. The interfering beams illuminate the substrate through a fused silica prism and a layer of index-matching liquid. The gratings with a period of 97 nm and line width of approximately 40 nm can be obtained by using a 257 nm light source. Solak[42] investigated the extreme ultraviolet lithography interferometry. Their system is based on undulator radiation from an electron storage ring and a Lloyd mirror interferometer. They have achieved 19 nm line and space patterns (37 nm pitch) Hence, the solid immersion lens has contributed to the advance of high-resolution lithography, but it is inconvenient to implement in practice as the optics need to be very close to the target material.

3. Far field laser interference lithography and laser direct writing for nanofabrication

1) Far field laser interference lithography

Laser-interference lithography (LIL) is a technique which can be applied for large-area, maskless, and noncontact nanofabrication. The main mechanism is that the

interference of two or more coherent light beams forms a horizontal standing-wave pattern[43,44]. It is suitable for the fabrication of repeatable structures such as periodic lines and 2D shapes. Figure 7 shows a typical schematic of the LIL experimental setup.

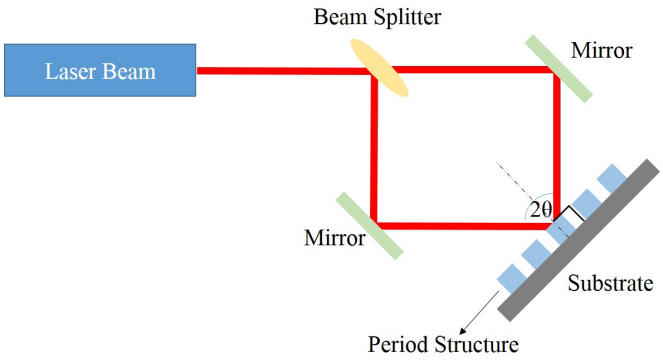

Figure 7 Schematic of the experimental setup for laser interference lithography.

Laser-interference lithography is suited for the fabrication of micro- and nano-structures in a large area. By overlapping exposures at different angles, various patterns can be produced, such as circular, square, and hexagonal geometry. Combining the LIL patterning and elastic stamp membrane transfer printing techniques, Seo [45] prepared large-area broadband photonic crystal membrane reflectors (MRs) on glass substrates. High-reflectivity broadband MRs on glass were fabricated with measured reflectivity of 95% around 1300 nm and a bandwidth of about 100 nm. Kawamura reported that two interfered infrared-femtosecond laser pulses with the wavelength of 800 nm were used to prepare two cross-superposed holographic gratings on silica glass[46]. By changing the energy density and the incidence angle of the irradiation laser beams, 1D or 2D arrays of holes or islands were fabricated. The smallest dimensions were a width of ~15 nm for lines and a diameter of ~20 nm for holes. Similarly, two-dimensional periodic microstructures

can also be prepared by a single shot of three interfered femtosecond laser pulses on the surface of silica glass[47]. Furthermore three types of complex micro/nanostructures were generated[48] on 6H-SiC crystal induced by arranging the types of three interferences femtosecond laser polarization combinations. To increase the flexibility of the technique and the complexity of the patterns, using multi-beam interferences is one solution. The simplest example is to use four beams, two oriented at ±θ in the x direction and two at ±θ in the y direction[49]. For example, four-beam nanosecond laser interference system[50] configuring different polarization modes was developed to generate periodic micro cone and hole structures on the surface. For the same purpose, Matsuo[51] described a novel microfabrication method based on interference of several coherent laser pulses in photosensitive media. This multi-beam interference method can be applied to write the periodic multidimensional interference patterns through periodic modulation of dielectric material, and it is potentially suitable for the photonic crystal fabrication based on photoresists, photosensitive glasses, and others.

2) Femtosecond laser direct writing

Using femtosecond lasers for the formation of nano-scale features is different from the conventional lasers. In fs laser, the laser interaction time (10^{-15}-10^{-13} s) is shorter than the time of electrons passing the energy to the lattice (around 10^{-11} s). So the fs laser can be used for cold machining, i.e., the laser energy is highly localized in the vicinity of focal point[52]. Controlling the laser fluence achieves the damaged effect that only the tip of laser beam is above the ablation or phase change threshold of the material, nanofabrication closing to the diffraction limit can be realized by a far field

femtosecond laser. This can be also understood by the multi-photon effect. One-photon absorption (OPA), two-photon absorption (TPA), or multi-photon absorption (MPA) often occur in the material processing when using high power density fs laser. Two photon absorption mechanisms are deplicted in Figure 8. In the figure, S_0, S_1, and S_2 stand for the ground state, one-photon allowed and two-photon allowed excited states, respectively. The incident light frequencies are ω_1 and ω_2 while the fluorescent emission frequency is ω_3. During standard optical lithography, the materials respond to light excitation to the first order effect. But for TPA and MPA the response is limited to two and higher orders. The required photon energy of TPA is certainly less than that of OPA. As a result, the volume involved in beam-material interaction reduces. This leads to a better resolution in writing the features. This effect is more obvious using the third order of the laser wavelength (λ^3) and high spatial resolution of the writing process (≦100 nm) beyond the optical diffraction limit is possible[53].

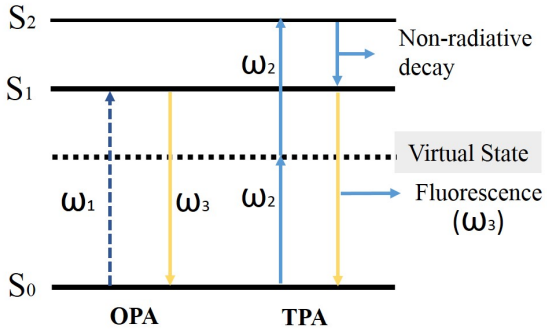

Figure 8 Schematic energy diagram of a TPA process.

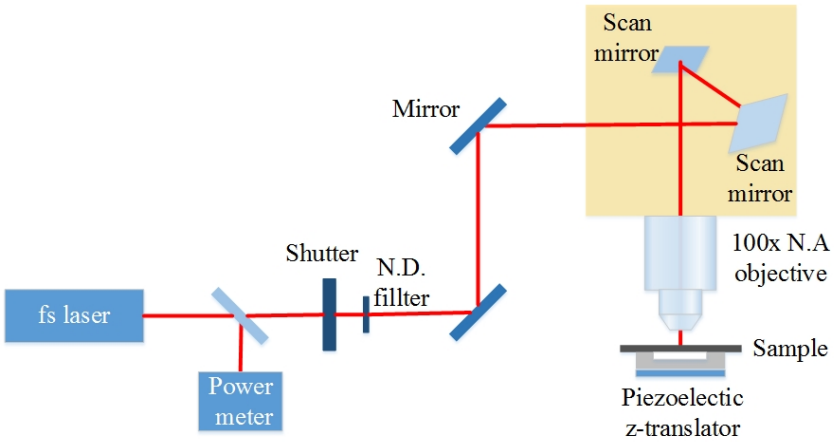

Figure 9 A typical DLW experimental set-up.

Figure 9 shows a typical DLW experimental setup. Femtosecond laser direct writing technique can be applied for fabrication of some devices. Viskadouros[54] reported the simple fabrication of flexible graphene-based field emission (FE) cathodes via direct laser writing, which emitting pixels on reduced graphene oxide (rGO) films deposited onto rGO:poly(3-hexylthiophene) (P3HT) composite layers. Laser processing also gives rise to a pronounced vertical alignment of rGO bundles perpendicular to the substrate. The laser-fabricated cathodes exhibit outstanding FE properties with a turn-on field of as low as 0.6 V/μm and a field enhancement factor of 8900.

Plasmonic lithography method based on two-SPP-absorption (TSPPA) was also proved to be useful for microfabrication induced by 800 nm femtosecond laser[55]. Resist patterns have been achieved with the period of 138 nm by exciting the SPP at the Al/resist interface with the 400 nm femtosecond laser[56]. The resolution mainly depends on the wavelength of the femtosecond pulses, the numerical aperture of the objective lens, the light intensity, the exposure time, and the sensitivity of the photopolymer. Kawata[57] and co-workers demonstrated that the diffraction limit could

be exceeded by non-linear effects. They achieved a subdiffraction-limit spatial resolution of 120 nm using 800 nm light. This shifts the working wavelength of photonic and optoelectronic devices into the visible and near-infrared regions. By introducing radical quenchers in the resin, the lateral spatial resolution was improved from the previously reported[58] value, 120 nm, to around 100 nm. The roughness measured from 10 μm×10 μm surface areas was averaged to 4-11 nm, which was slightly affected by the laser pulse energy but independent on the scanning pitch when it was smaller than a critical value. Then a higher lateral resolution of 80 nm (corresponding to λ/10) was achieved by increasing the linear scan speed around the exposure threshold of an optimized photopolymer containing a highly sensitive and efficient photoinitiator[59]. By reducing the wavelength of a femtosecond laser to 520 nm, nanoscale features as small as 65 +/- 5 nm have been formed[60], indicating that sub-diffraction limited line widths are obtained in both cases. Using bridge-like structures[61], fine lines with sub-25-nm width were produced by controlling the incident laser power and the scan speed of a femtosecond pulsed laser beam at a wavelength of 780 nm in the commercial urethane acrylate resin SCR-500. Two-photon lithography in negative SU-8 photoresist was developed to fabricate mechanically stable, stress-free, extended nanorods having lateral sizes of about 30 nm[62]. The high resolution is achievable with the given combination of materials and fabrication techniques, which demonstrates its potential for the fabrication of large-scale nanostructures at visible wavelengths.

Until now, 2PPL facilitates writing features with lateral sizes of 90 nm[63], 80

nm[64,65], and 65 nm[60] when 1030 nm, 800 nm, and 520 nm pulsed lasers are used respectively for two-photon excitation polymerization. The feature sizes are already below the diffraction limit because of an intrinsic chemical nonlinearity.

4. Laser manufacturing of nano materials and micro-nanodevices

1) Laser manufacturing of nanomaterials

Nanomaterials have unique physical and chemical properties. Nanomaterials can be manufactured by several approaches. Various laser-based methods have been developed for the fabrication of nanomaterials including laser ablation, laser exfoliation and laser-assisted reduction. Most laser-based methods are easily scalable and therefore applicable for large scale nanoparticle (NP) synthesis. However, they are restricted in numerical parameters, such as processing efficiency, material variety and dispersability of the nanoparticles in liquid media. Furthermore, for many applications, purification steps such as centrifugation are required to remove chemical by-products[66,67] and the quality and purity of nanoparticles produced by nonlaser based approaches are insufficient. Therefore, in the last two decades laser-based synthesis techniques for NP generation have been developed. The most laser-based NP synthesis techniques are based on laser ablation of solid targets which in a gas, vacuum or liquid environment[68]. Figure 10 shows a schematic diagram of nanoparticle generation by laser ablation.

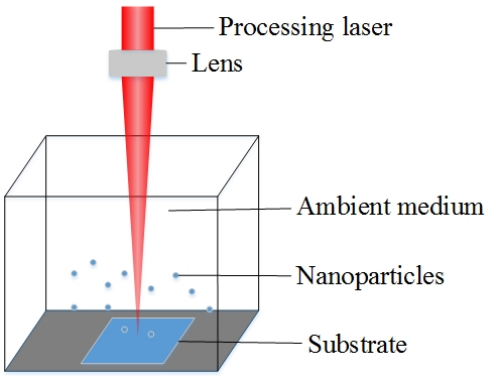

Figure 10 Schematic diagram of nano particle generation by laser ablation.

Kuznetsov et al.[69] presented a novel method for high-speed fabrication of large scale periodic arrays of nanoparticles. The diameters of the nanoparticles range from 40 to 200 nm. This method is based on a combination of nanosphere lithography and femtosecond laser-induced transfer. An important advantage of this method is that the size distribution of the fabricated nanoparticles can be controlled from a few hundred of nanometers to tens of nm. This method provides a minimum theoretical particle diameter of 10 nm for spherical nanoparticles, which is comparable to the size of nanoparticles produced by chemical methods in solutions.

Also carbon nanotubes (CNTs) can be produced by laser ablation. The method by laser synthesis of CNTs was given by Guo et al.[70]. Then pulsed laser deposition (PLD) has become one of the most powerful and adaptive methods to fabricate CNTs[71,72]. The CNTs from the MWCNT thin film has diameters of approximately 10 nm and retaining their general multi-walled structure along the length of the tubes. Recently, a new laser material-transfer scheme was reported [73] for transfer printing both the silver-paste and CNT thin film in pattern simultaneously. Unlike conventional laser transfer techniques, this transfer method can transfer materials on the unexposed locations. Besides CNTs, TiO_2 nanotube (TNT) films[74], Si and Ge

nanowires[75,76,77] based on laser assisted vapor–liquid–solid (VLS) mechanism. The nanowires with diameters as small as 60 nm are produced by the interference between incident laser radiation and surface scattered radiation within a diffraction limited spot, which causes spatially confined, periodic heating needed for high resolution CVD. The diameter of the silicon nanowires is far below the diffraction limit of the laser wavelength of 395 nm. And the nanowire is directly fabricated on an insulating surface which ready for subsequent device fabrication without the need for transfer and alignment. Thus greatly simplifying device fabrication processes.

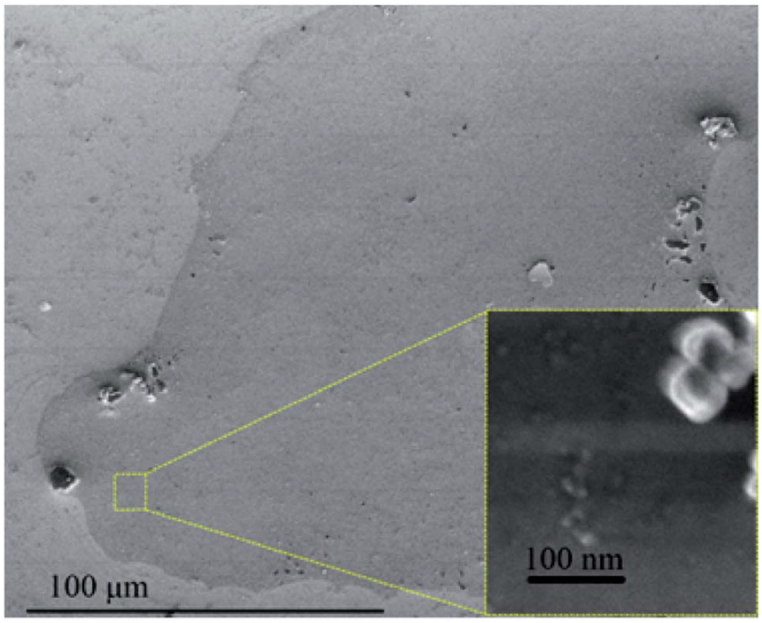

Figure 11 SEM image of a layer obtained after fs laser ablation of highly oriented pyrolytic graphite in liquid N_2. The inset shows a magnification of the area inside the yellow dashed box[78].

An important progress is the synthesis of graphene and other 2D materials with laser techniques. Russo et al.[78] reported a laser exfoliation of porous graphene in liquid with femtosecond laser irradiation of highly oriented pyrolytic graphite. Figure 11 shows tens micrometer size porous graphene fabricated with femtosecond laser in liquid N_2. A femtosecond laser induced coal gasification is regarded as the dominant

mechanism[79]. It is possible to get high quality graphene by laser exfoliation with well-controlled laser parameters[80,81].

2) Femtosecond laser-induced nanojoining

Welding and joining is an essential step in the fabrication of various devices and functional systems on the macroscale, microscale and nanoscale. As devices become increasingly smaller, challenges faced in microjoining and nanojoining must be overcome before these joints are safely implemented[82]. Various approaches have been developed for nanojoining, such as e-beam bombardment[83], focusing ion beam deposition[84], Joule heating of electrical currents[85], ultrasonic welding[86], vacuum brazing[87] and nanosoldering with low melting point solders[88]. In addition, laser is also be used for nanojoining. Picosecond laser pulses have been employed to join or to weld gold nanoparticles on carbon-coated copper grids[89]. Surfactant-free gold nanospheres (diameter = 9.3 nm) were successfully nanowelded by irradiating laser pulses of 532 nm and 0.2 mJ for 10min on a carbon-coated copper TEM grid. It indicated that gold nanoparticles are welded in a single phase to have ohmic nanocontact. Similarly, Gold nanoparticles have been joined using Ag nanoparticles[90] to fabricate nanowires by irradiating gold nanospheres of 25 nm in diameter and silver nanospheres of 8 nm in diameter held together on a carbon-coated copper grid with a 30 ps laser pulse of 532 nm for 20 min at a fluence of 3.0 mJ/cm^2. The excitation of the surface plasmon resonances of the base-metallic gold nanospheres paves the way for the silver nanojoining of gold nanoparticles rather than the filler-metallic silver nanospheres.

Compared to picosecond laser irradiation, femtosecond laser irradiation can result in an ultrafast and almost nonthermal melting of solid materials, which is promising for developing novel joining technologies for nano- and/or molecular devices[91]. Hu et al.[91] reported that femtosecond laser irradiation at a proper intensity results in the welding of most Au nanoparticles while avoiding photonic fragmentation. They observed two effects by femtosecond laser irradiation: the generation of large number of tiny nanoparticles with a diameter of 1~3 nm and welding of 2~3 Au nanoparticles with a size around 15 nm. By adjusting the femtosecond laser pulse fluence during irradiation of PVP coated Ag NPs in aqueous solution[92], it is feasible to control the separation and bonding within networks of Ag NPs. Nanojoining leads to the formation of metallic connection between noble metallic nanoparticles. Hu et al.[93] also reported that the welded Au nanoparticles can work effectively for surface enhanced Raman spectroscopy. They also observed that direct irradiation of Ag foil can induce nanopatterns on the surface, and those nanostructures can also work for the probe of surface enhanced Raman spectroscopy and plasmonic devices[94]. Recently, they successfully display that silver nanowires can be welded with femtosecond laser irradiation without the shape of nanowires. They attributed this phenomenon to femtosecond laser induced surface melting[95]. Figure 12 shows the nanowelded Au nanoparticles by femtosecond laser irradiation.

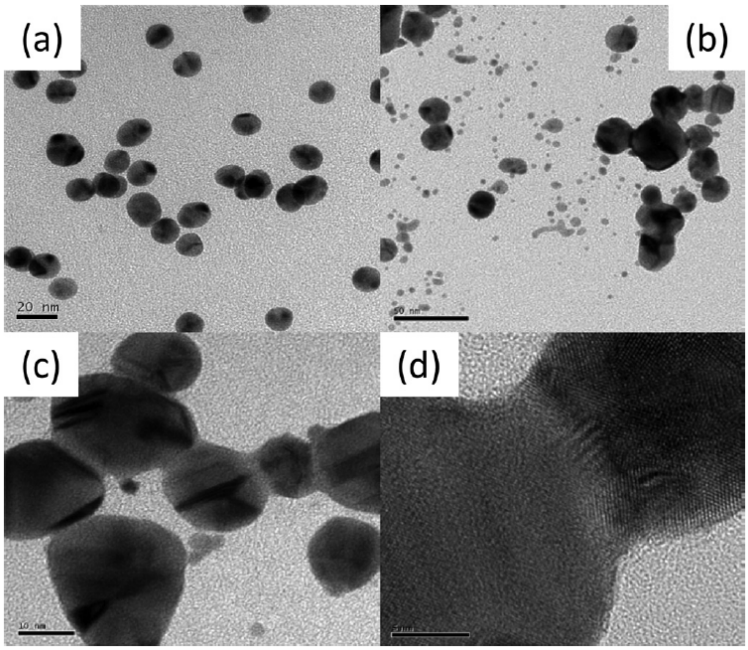

Figure 12 Nanowelded Au nanoparticles by femtosecond laser irradiation. (a) Pristine liquid, (b) irradiation at an intensity of 4×10^{14} W/cm^2, (c) irradiation at 3×10^{10} W/cm^2, and (d) local structures of typical welded necks between two particles shown in (c)[94].

In addition to the same metal nanoparticles, the nanojoining of different metal nanoparticles were also reported by Liu et al.[96]. They presented an effective way to join Pt-Ag nanoparticles with nano Ag filler metal by femtosecond laser irradiation. And the nano brazed interface between Pt-Ag and Ag showed good lattice matching along (111)Ag//(111)Ag-Pt. By femtosecond laser irradiation, Al-Fe nanoparticles were joined successfully[97]. The results showed that the nanostructure of Al NPs was monocrystalline after deposition, while that of Fe NPs was polycrystalline. These structures were retained after fs irradiation at fluences of 1.3 mJ/cm^2. Meanwhile, nanojoining is in very early stages of development. It requires the assembly of micro/nano structures of same and different materials to a higher degree of accuracy and requires further investigation on thermodynamic and dynamic properties of nanoparticles. Suitable nanojoining technologies are necessary for future

nano-manufacturing process chains.

3) Laser writing of embedded microlenses

Microlenses and microlens arrays, as important Micro-optics devices, have been applied widely in optical beam shaping[98], optical sensors[99], wide angle imaging[100], microelectromechanical systems (MEMS)[101], and enhancing the light coupling efficiency of light-emitting diodes (LEDs)[102] and charge-coupled devices (CCDs)[103] in parallel micro-optic manufacturing. However, microlenses fabricated by surface manufacturing are easily scratched and difficult to obtain alignments beyond submillimeter scales when are integrated with optical systems. But the cavity microball lens (CMBL) can alleviate these issues. Femtosecond laser, as an optimum selection to fabricate CMBL, could be strictly confined inside the material due to a nonlinear and multiphoton nature of the interaction with the materials. Chong et al.[104] successfully fabricated CMBLs inside PMMA slices using heat-accumulated ablation driven by high repetition rate femtosecond fiber laser pulses, shown in Figure 13. The micro-telescope combined with a CMBL displays the super-wide angle imaging (350°). The fabrication technique of CMBL via using femtosecond laser is a simple and rapid process and can gain good optical properties, including the effective focal length and viewing angles. Lu et al.[105] also reported the fabrication of solvent-tunable polydimethylsiloxane (PDMS) microlenses using the femtosecond laser direct writing (FsLDW) technique. PDMS microlenses with equation-defined profiles have been fabricated according to preprogrammed models which including both spherical microlens and aspherical hyperboloid microlens. In addition to excellent optical

performance derived from the high accuracy and smooth surface, the resultant PDMS microlenses also show unique solvent-tunable properties.

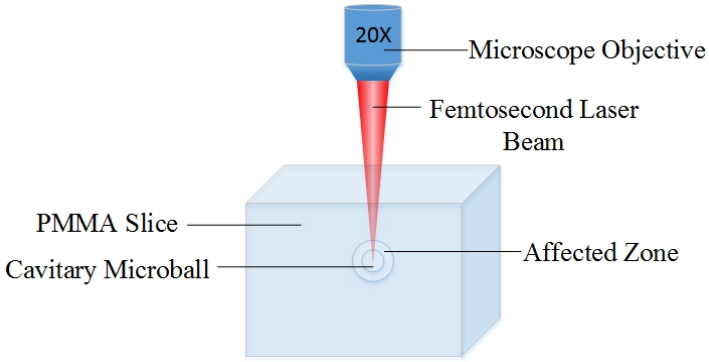

Figure 13 Schematic of the formation of the CMBL fabricated using the focused ablation of a femtosecond laser. Adapted from ref.104.

5. Stimulated-emission-induced depletion (STED) assisted laser fabrication

1) STED lithography

The stimulated emission depletion (STED) was designed for the use of super resolution far-field imaging. In 1994, Hell and Wichmann[106] provided a way to break the limitation of the resolution in optical microscopy[107]. In their proposal, they argued that the resolution in fluorescence microscopy can be overcome the diffraction limitation. If the fluorescence in the outer rim of the diffraction-limited point spread function (PSF) of the excitation beam can be switched off quickly enough so that the outer fluorophores cannot emit a photon, according to this conception, the inner fluorophore can display a sub-Abbe resolution imaging[108]. This turn-off can be realized by stimulated emission. This is the so-called stimulated emission depletion mechanism. Figure 14 shows typical setups for STED microscopy and STED inspired lithography.

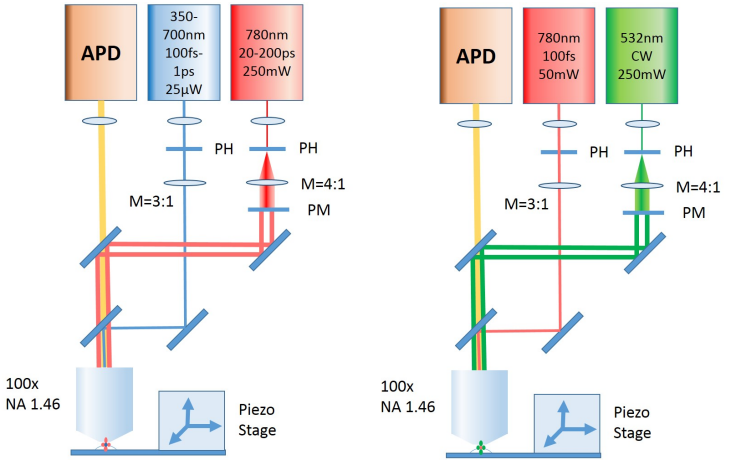

Figure 14 Typical setups for STED microscopy (left) and STED lithography (right). Adapted from ref. 109.

The basic idea of this STED-inspired nano-manufacturing method is that the fluorophores can be excited by the conventional laser beam. Then a donut-shaped depletion laser beam with a longer wavelength is used to de-excite the peripheral fluorescence through stimulated emission. Under the influence of this effect thus only fluorescence emission from the sub-diffraction-limited center is left out to be recorded.

Wolf [110] reported femtosecond pump-probe experiments on two different photoinitiators in solution. For the purpose of beating Abbe's diffraction limit, these two molecules have recently appeared as attractive candidates for far-field optical lithography based on STED inspired approaches. They find that stimulated emission clearly dominates over excited-state absorption by the use of 7-diethylamino-3-thenoylcoumarin (DETC), whereas the opposite holds true for the case of isopropylthioxanthone (ITX). They claimed that as depletion mechanism in STED photoresists it is desirable that stimulated emission dominates over excited-state absorption. Thus, DETC is an attractive photoinitiator.

2) STED inspired direct laser writing

Adding stimulated emission depletion (STED) to direct laser writing (DLW) can integrate advantages from both STED and DLW. STED-inspired diffraction unlimited DLW has been realized[111]. One laser pulse is used to excite photo-initiators for radical polymerization, and a second laser is used locally to inhibit the photo-initiator of the polymerization in the outer rim of the point spread function (PSF). Thereby, polymerization is only reacted in regimes within the outer PSF. Based on the STED approach, two-photon polymerization can be combined with STED mechanisms to process structures with feature sizes below the diffraction limit. Figure 15 shows schematic representation of lateral localization and resolution in microscopy, DLW and STED-DLW. Combination of STED and DLW can be used for three dimensions manufacturing. Experiments translating of diffraction unlimited optical laser-scanning microscopy to optical direct-laser-writing lithography in three dimensions has been successfully presented by Fischer[111,112].

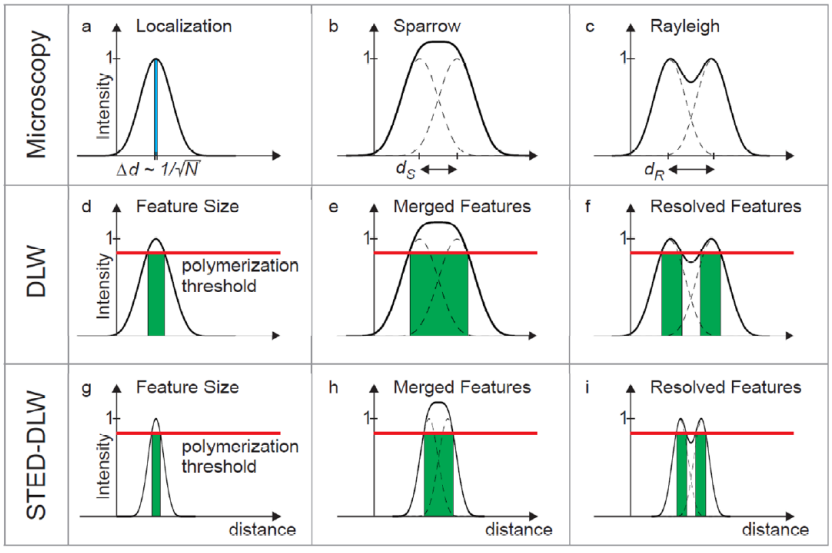

Figure 15 Schematic representation of lateral localization and resolution in microscopy (a-c), DLW (d-f) and STED-DLW (g-i)[113].

A novel photoresist (composed of pen-taerythritol triacrylate and isopropyl thioxanthone) was used that favors stimulated emission depletion by a π-π* transition in the photoinitiator and an excitation wavelength of λ= 810 nm was used for a two-color two-photon excitation scheme, they have achieved 65 nm= λ/12.5 wide lines. This value is significantly smaller than a 155 nm width for a zero depletion power. Further improvements and optimization will require tuning the optical transitions of the photoresist to reduce parasitic two-photon excitation of the continuous-wave depletion beam. Hence, the diffraction limit becomes less and less a relevant barrier for line-width reductions in three dimensions optical lithography. How to design a novel photoresist material system which can support for STED lithography with the size of sub 10 nm becomes a demanding. It is very highly rewarding topic for materials science and super-resolution nanomanufacturing. In 2014, the mechanisms of polymerization initiation and photoinhibition in DETC-containing photoresists were investigated also by STED DLW[114]. The fluorescence from the DETC molecules was investigated under writing conditions with different repetition rates and also different pulsed depletion with various pulse delays. The results show a two-photon absorption and a weak one-photon anti-Stokes excitation with the picosecond ring-shaped depletion laser.

Yuan[115] fabricated nanodots in resist with initiator of isopropyl thioxanthone (ITX) (81 nm in diameter and nanoline of 93 nm in width). In their experiment, an 800 nm, 75-MHz fs laser was used as the polymerization light and a 532 nm donut mode continuous wave (CW) laser was used as the depletion light. This technology is

useful for simplifying super resolution STED DLW. Cao[116] used an ethoxylated bis-phenol-A dimethacrylate based photoresin BPE-100 with relatively high photosensitivity and modulus for the creation of sub-50 nm features, where the direct laser writing technique is based on the single-photon photoinhibited polymerization. Overlapping two laser beams with different wavelengths was used for wavelength-controlled activation of photoinitiating and photoinhibiting processes in the polymerization. They achieve 40 nm dots and a minimum line width of 130 nm in the super-resolution fabrication technique based on the photoinhibited polymerization of photoresin BPE-100. Applying a film of thermally stable photochromic molecules above the photoresist, Andrew[117] demonstrated lines with an average width of 36 nm, about one-tenth of the illuminating wavelength λ_1 = 325 nm. Simultaneous irradiation of a second wavelength, λ_2= 633 nm, renders the film opaque to the writing beam except at nodal sites, which allowing subdiffractional patterning. The three-dimensional optical beam lithography with 9 nm feature size and 52 nm two-line resolution was reported by Gan[118], using a newly developed two-photon absorption resin with high mechanical strength. This evidences that an e-beam style resolution of the feature size can be reached by STED-DLW. These studies are paving the way towards low-cost three-dimensional maskless laser direct writing with resolution fully comparable to electron beam lithography.

6. Summary and outlooks

Laser manufacturing of nanostructures is still in the basic research phase. While

the near field methods can provide very high resolutions (20-100 nm), they are basically a surface processing method. The near field processing is inconvenient to implement in practice as the optics need to be very close (20 nm-1μm) to the target material. The far field techniques have greater promises if the resolution can be consistently improved comparable to that of electron beams or focused ion beams. Nano-joining is also in a very early stage of development. It requires the assembly of micro/nanoscale building blocks at a higher degree of accuracy. A nano-manipulation tool is still not well established yet. Laser direct writing of polymeric 3D nanostructures is dominated by the "bottom up" approach based on the TPP method. It is reliable and mature, and ready for commercial applications. However, this method has not developed for other materials, such as metal. The STED assisted laser fabrication has the advantages of geometric freedom (up to 3D lithography), simply operating and low cost as laser direct writing. The record resolutions in STED and STED-related lithography techniques has reached a range of some tens of nanometers, far below the wavelength of visible light. However, STED-lithography setups are not yet widely available especially in material science.

However, two-photon lithography setups are commercially available, and an upgrade to a STED lithography setup is straightforwardly achieved by applying a low-cost CW STED laser such as a semiconductor laser as the depletion laser. Moreover, continuous developments of laser technology has lowed the cost of femtosecond lasers for two-photon excitation as well as for pulsed STED.

Each technique for nanofabrication has certain characteristic advantages and

drawbacks. It is a way to combine two or more methods to implement the required nanomanufacturing. We consider STED combination with nonlinear effects as an ideal candidate for nanomanufacturing with a molecular level resolution. Until now, the key challenges for STED laser manufacturing of micro- and nano-structures is to apply for materials other than polymers. If nanostructures could be made with feature sizes of 10 nm in all three dimensions with different materials, a dream of nanorobotic world would eventually come true.

Acknowledgement:

The study is partially supported by the Beijing Oversea High-Level Talent Project and a strategic research grant (KZ20141000500, B-type) of Beijing Natural Science Foundation, P. R. China. We appreciate the research initiative funding provided by the University of Tennessee as a new hire package to AH.

References

[1] Y. Chen, A. Pepin. Electrophoresis 22(2) (2001) 187-207.
[2] D. S. Engstrom, B. Porter, M. Pacios, H. Bhaskaran, Journal of Materials Research 29(17) (2014) 1792-1816.
[3] L. Li, M. Hong, M. Schmidt, M. Zhong, A. Malshe, B. Huis, V. Kovalenko, CIRP Annals-Manufacturing Technology 60(2) (2011) 735-755.
[4] D. Mailly, The European Physical Journal-Special Topics 172(1) (2009) 333-342.
[5] M. M. Alkaisi, R. J. Blaikie, S. J. McNab, R. Cheung, D. R. S. Cumming, Applied Physics Letters 75(22) (1999) 3560-3562.
[6] R. J. Blaikie, M. M. Alkaisi, S. J. McNab, D. R. S. Cumming, R. Cheung, D. G. Hasko, Microelectronic engineering 46(1) (1999) 85-88.
[7] J. C. Martinez-Anton, Journal of Optics A: Pure and Applied Optics 8(4) (2006) S213.
[8] J. K. Chua, V. M. Murukeshan, S. K. Tan, Q. Y. Lin, Optics express 15(6) (2007) 3437-3451.
[9] E. A. Bezus, L. L. Doskolovich, N. L. Kazanskiy, Microelectronic Engineering 88(2) (2011) 170-174.
[10] V. M. Murukeshan, J. K. Chua, S. K. Tan, Q. Y. Lin, Optical Engineering 47(12) (2008) 129001-129001.
[11] W. Srituravanich, N. Fang, C. Sun, Q. Luo, X. Zhang, Nano letters 4(6) (2004) 1085-1088.
[12] X. Luo, T. Ishihara, Optics Express 12(14) (2004) 3055-3065.
[13] Z. W. Liu, Q. H. Wei, X. Zhang, Nano Letters 5(5) (2005) 957-961.
[14] E. S. Kim, K. C. Choi, IEEE Transactions on 13(2) (2014) 203-207.
[15] T. Xu, Y. Zhao, J. Ma, C. Wang, J. Cui, C. Du, X. Luo, Optics express 16(18) (2008) 13579-13584.
[16] K. V. Sreekanth, J. K. Chua, V. M. Murukeshan, Applied optics 49(35) (2010) 6710-6717.
[17] J. W. Kingsley, S. K. Ray, A. M. Adawi, G. J. Leggett, D. G. Lidzey, Applied Physics Letters 93(21) (2008) 213103.
[18] S. Sun, G. J. Leggett, Nano letters 2(11) (2002) 1223-1227.
[19] S. Sun, G. J. Leggett, Nano Letters 4(8) (2004) 1381-1384.
[20] T. H. Dam, P. Pantano, Review of scientific instruments 70(10) (1999) 3982-3986.
[21] G. Krausch, S. Wegscheider, A. Kirsch, H. Bielefeldt, J. C. Meiners, J. Mlynek, Optics communications 119(3) (1995) 283-288.
[22] C. P. Grigoropoulos, D. J. Hwang, A. Chimmalgi, MRS bulletin 32(01) (2007) 16-22.
[23] M. Kuwahara, T. Nakano, J. Tominaga, M. B. Lee, N. Atoda, Japanese journal of applied physics 38(9A) (1999) L1079.
[24] H. A. Bethe, Physical Review 66(7-8) (1944) 163.
[25] N. Murphy-DuBay, L. Wang, X. Xu, Applied Physics A 93(4) (2008) 881-884.
[26] X. Xu, E. X. Jin, S. M. Uppuluri, In Optical Science and Technology, the SPIE 49th Annual Meeting (2004) 230-243 International Society for Optics and Photonics.
[27] J. Xu, J. Wang, Q. Tian, In Photonics Asia 2004 (2005) 284-291 International Society for Optics and Photonics.
[28] L. Wang, S. M. Uppuluri, E. X. Jin, X. Xu, Nano letters 6(3) (2006) 361-364.
[29] X. Wen, L. M. Traverso, P. Srisungsitthisunti, X. Xu, E. E. Moon, Applied Physics A 117(1) (2014) 307-311.
[30] S. Uppuluri, E. C. Kinzel, Y. Li, X. Xu, Optics express 18(7) (2010) 7369-7375.
[31] C. Huber, A. Trügler, U. Hohenester, Y. Prior, W. Kautek, Physical Chemistry Chemical Physics 16(6) (2014) 2289-2296.
[32] W. Guo, Z. B. Wang, L. Li, D. J. Whitehead, B. S. Luk'yanchuk, Z. Liu, Applied physics letters 90(24) (2007) 243101.
[33] M. Hasegawa, T. Ikawa, M. Tsuchimori, O. Watanabe, Y. Kawata, Macromolecules 34(21) (2001) 7471-7476.
[34] T. Sakai, Y. Tanaka, Y. Nishizawa, M. Terakawa, M. Obara, Applied Physics A 99(1) (2010) 39-46.
[35] D. Brodoceanu, L. Landström, D. Bäuerle, Applied Physics A 86(3) (2007) 313-314.

[36] N. Nedyalkov, T. Sakai, T. Miyanishi, M. Obara, Journal of Physics D: Applied Physics 39(23) (2006) 5037.
[37] D. A. Fletcher, K. B. Crozier, C. F. Quate, G. S. Kino, K. E. Goodson, D. Simanovskii, D. V. Palanker, Applied Physics Letters 77(14) (2000) 2109-2111.
[38] T. Kim, W. S. Lee, H. E. Joe, G. Lim, G. J. Choi, M. G. Gang, N. C. Park, Applied Physics Letters 101(16) (2012) 161109.
[39] K. S. Park, T. Kim, W. S. Lee, H. E. Joe, B. K. Min, Y. P. Park, N. C. Park, Japanese Journal of Applied Physics 51(8S2) (2012) 08JF01.
[40] T. Milster, T. Chen, D. Nam, T. E. Schlesinger, In Photomask Technology (2004) 545-556 International Society for Optics and Photonics.
[41] J. A. Hoffnagle, W. D. Hinsberg, M. Sanchez, F. A. Houle, Journal of Vacuum Science & Technology B 17(6) (1999) 3306-3309.
[42] H. H. Solak, D. He, W. Li, F. Cerrina, Journal of Vacuum Science & Technology B 17(6) (1999) 3052-3057.
[43] S. Bai, W. Zhou, C. Tao, K. D Oakes, A. Hu, Current Nanoscience 10(4) (2014) 486-496.
[44] S. Bai, W. Zhou, Y. Lin, Y. Zhao, T. Chen, A. Hu, W. W. Duley, Journal of nanoparticle research 16(7) (2014) 1-14.
[45] J. Park, D. Zhao, IEEE Photonics journal 5(1) (2013) DOI: 10.1109/JPHOT.2012.2236545.
[46] K. I. Kawamura, N. Sarukura, M. Hirano, N. Ito, H. Hosono, Applied Physics Letters 79(9) (2001) 1228-1230.
[47] Z. Guo, S. Qu, L. Ran, Y. Han, S. Liu, Optics letters 33(20) (2008) 2383-2385.
[48] X. Jia, T. Q. Jia, L. E. Ding, P. X. Xiong, L. Deng, Z. R. Sun, Z. G. Wang, J. R. Qiu, Z. Z. Xu, Optics letters 34(6) (2009) 788-790.
[49] S. R. J. Brueck, Proceedings of the IEEE 93(10) (2005) 1704-1721.
[50] D. Wang, Z. Wang, Z. Zhang, Y. Yue, D. Li, R. Qiu, C. Maple, Journal of Applied Physics 115(23) (2014) 233101.
[51] S. Matsuo, T. Kondo, S. Juodkazis, V. Mizeikis, H. Misawa, In Symposium on Integrated Optoelectronic Devices (2002) 327-334 International Society for Optics and Photonics.
[52] A. Hu, M. Rybachuk, Q. B. Lu, W. W. Duley, Applied Physics Letters 91(13) (2007) 131906.
[53] K. Takada, H. B. Sun, S. Kawata, Applied Physics Letters 86(7) (2005) 071122.
[54] G. Viskadouros, D. Konios, E. Kymakis, E. Stratakis, Applied Physics Letters 105(20) (2014) 203104.
[55] Y. Li, F. Liu, L. Xiao, K. Cui, X. Feng, W. Zhang, Y. Huang, Applied Physics Letters 102(6) (2013) 063113.
[56] Y. Li, F. Liu, Y. Ye, W. Meng, K. Cui, Feng, et al. Applied Physics Letters 104(8) (2014) 081115.
[57] S. Kawata, H. B. Sun, T. Tanaka, K. Takada, Nature 412(6848) (2001) 697-698.
[58] K. Takada, H. B. Sun, S. Kawata, Applied Physics Letters 86(7) (2005) 071122.
[59] J. F. Xing, X. Z. Dong, W. Q. Chen, X. M. Duan, N. Takeyasu, T. Tanaka, S. Kawata, Applied physics letters 90(13) (2007) 131106-131106.
[60] W. Haske, V. W. Chen, J. M. Hales, W. Dong, S. Barlow, S. R. Marder, J. W. Perry, Optics express 15(6) (2007) 3426-3436.
[61] D. Tan, Y. Li, F. Qi, H. Yang, Q. Gong, X. Dong, X. Duan, Applied physics letters 90(7) (2007) 071106-071106.
[62] S. Juodkazis, V. Mizeikis, K. K. Seet, M. Miwa, H. Misawa, Nanotechnology 16(6) (2005) 846.
[63] F. Burmeister, S. Steenhusen, R. Houbertz, U. D. Zeitner, S. Nolte, A. Tünnermann, Journal of Laser Applications 24(4) (2012) 042014.
[64] J. F. Xing, X. Z. Dong, W. Q. Chen, X. M. Duan, N. Takeyasu, T. Tanaka, S. Kawata, Applied physics letters 90(13) (2007) 131106-131106.
[65] V. F. Paz, M. Emons, K. Obata, A. Ovsianikov, S. Peterhänsel, K. Frenner, et al. Journal of Laser Applications 24(4) (2012) 042004.
[66] A. Hahn, S. Barcikowski, B. N. Chichkov, Pulse 40(45) (2008) 50.
[67] A. Hahn, S. Barcikowski, J Laser Micro/Nanoeng 4 (2009) 51-54.
[68] D. S. Burgess, Photonics Spectra 1 (2001) 26–29.
[69] A. I. Kuznetsov, A. B. Evlyukhin, M. R. Gonçalves, C. Reinhardt, A. Koroleva, M. L.

Arnedillo, et al., Acs Nano, 5(6) (2011) 4843-4849.
[70] T. Guo, P. Nikolaev, A. G. Rinzler, D. Tomanek, D. T. Colbert, R. E. Smalley, The Journal of Physical Chemistry 99(27) (1995) 10694-10697.
[71] F. Bonaccorso, C. Bongiorno, B. Fazio, P. G. Gucciardi, O. M. Marago, A. Morone, C. Spinella, Applied Surface Science 254(4) (2007) 1260-1263.
[72] A. A. Stramel, M. C. Gupta, H. R. Lee, J. Yu, W. C. Edwards, Optics and lasers in Engineering 48(12) (2010) 1291-1295.
[73] H. Y. Liao, J. R. Ho, S. K. Chang-Jian, Journal of Display Technology 10(12) (2014) 1083-1087.
[74] J. A. Losilla, C. Ratanatawanate, K. J. Balkus Jr, Journal of Experimental Nanoscience 9(2) (2014) 126-137.
[75] A. M. Morales, C. M. Lieber, Science 279(5348) (1998) 208-211.
[76] J. I. Mitchell, N. Zhou, W. Nam, L. M. Traverso, X. Xu, Scientific reports 4 (2014)..
[77] W. Nam, J. I. Mitchell, D. Y. Peide, X. Xu, Nanotechnology 26(5) (2015) 055306.
[78] P. Russo, A. Hu, G. Compagnini, W. W. Duley, N. Y. Zhou, Nanoscale 6(4) (2014) 2381-2389.
[79] P. Russo, A. Hu, G. Compagnini, Nano-micro letters 5(4) (2013) 260-273.
[80] M. Qian, Y. S. Zhou, Y. Gao, T. Feng, Z. Sun, L. Jiang, Y. F. Lu, Applied Surface Science 258(22) (2012) 9092-9095.
[81] P. Kumar, RSC Advances 3(30) (2013) 11987-12002.
[82] A. Hu, Y. Zhou, W. W. Duley, significance 9 (2011) 10.
[83] S. Xu, M. Tian, J. Wang, J. Xu, J. M. Redwing, M. H. Chan, Small 1(12) (2005) 1221-1229.
[84] A. V. Krasheninnikov, K. Nordlund, J. Keinonen, F. Banhart, Physical Review B 66(24) (2002) 245403.
[85] A. Vafaei, A. Hu, I. A. Goldthorpe, Nano-Micro Letters 6(4) (2014) 293-300.
[86] Y. Zhou, A. Hu, M. I. Khan, W. Wu, B. Tam, M. Yavuz, In Journal of Physics: Conference Series 165(1) (2009) 012012.
[87] W. Wu, A. Hu, X. Li, J. Q. Wei, Q. Shu, K. L. Wang, et al. Materials letters 62(30) (2008) 4486-4488.
[88] Y. Peng, T. Cullis, B. Inkson, Nano letters 9(1) (2008) 91-96.
[89] S. J. Kim, D. J. Jang, Applied Physics Letters 86(3) (2005) 033112.
[90] M. Son, S. J. Kim, J. Y. Kim, D. J. Jang, Journal of nanoscience and nanotechnology 13(8) (2013) 5777-5782.
[91] A. Hu, S. K. Panda, M. I. Khan, Y. Zhou, Chin J Lasers 36 (2009) 3149-3159.
[92] H. Huang, L. Liu, P. Peng, A. Hu, W. W. Duley, Y. Zhou, Journal of Applied Physics 112(12) (2012) 123519.
[93] A. Hu, W. W. Duley, Chemical Physics Letters 450(4) (2008) 375-378.
[94] A. Hu, P. Peng, H. Alarifi, X. Y. Zhang, J. Y. Guo, Y. Zhou, W. W. Duley, Journal of Laser Applications 24(4) (2012) 042001.
[95] A. Hu, G. L. Deng, S. Courvoisier, O. Reshef, C. C. Evans, E. Mazur, Y. Zhou, In SPIE NanoScience+ Engineering (2013) 880907-880907 International Society for Optics and Photonics.
[96] L. Liu, H. Huang, A. Hu, G. Zou, L. Quintino, Y. Zhou, Nano-Micro Letters 5(2) (2013) 88-92.
[97] Z. Jiao, H. Huang, L. Liu, A. Hu, W. Duley, P. He, Y. Zhou, Journal of Applied Physics 115(13) (2014) 134305.
[98] A. Bu, U. D. Zeitner, Optical Engineering 41(10) (2002) 2393-2401.
[99] N. Lindlein, J. Pfund, J. Schwider, Optical Engineering 40(5) (2001) 837-840.
[100] Q. Dai, R. Rajasekharan, H. Butt, X. Qiu, G. Amaragtunga, T. D. Wilkinson, Small 8(16) (2012) 2501-2504.
[101] C. P. B. Siu, H. Zeng, M. Chiao, Optics express 15(18) (2007) 11154-11166.
[102] E. Wrzesniewski, S. H. Eom, W. Cao, W. T. Hammond, S. Lee, E. P. Douglas, J. Xue, Small, 8(17) (2012) 2647-2651.
[103] M. E. Motamedi, M. P. Griswold, R. E. Knowlden, In San Diego,'91, San Diego, CA (1991). 22-32) International Society for Optics and Photonics.
[104] C. Zheng, A. Hu, K. D. Kihm, Q. Ma, R. Li, T. Chen, W. W. Duley, Small. (2015) DOI: 10.1002/smll.201403419.

[105] D. X. Lu, Y. L. Zhang, D. D. Han, H. Wang, H. Xia, Q. D. Chen, H. B. Sun, J. Mater. Chem. C. 3 (2015) 1751-1756.
[106] S. W. Hell, J. Wichmann, Optics letters 19(11) (1994) 780-782.
[107] E. Abbe, Archiv für mikroskopische Anatomie 9(1) (1873) 413-418.
[108] T. A. Klar, S. W. Hell, Optics letters 24(14) (1999) 954-956.
[109] T. A. Klar, R. Wollhofen, J. Jacak, Physica Scripta 2014(T162) (2014) 014049.
[110] T. J. Wolf, J. Fischer, M. Wegener, A. N. Unterreiner, Optics letters 36(16) (2011) 3188-3190.
[111] J. Fischer, G. von Freymann, M. Wegener, Advanced materials 22(32) (2010) 3578-3582.
[112] J. Fischer, M. Wegener, Advanced Materials 24(10) (2012) 65-69.
[113] R. Wollhofen, J. Katzmann, C. Hrelescu, J. Jacak, T. A. Klar, Optics express 21(9) (2013) 10831-10840.
[114] J. Fischer, J. B. Mueller, A. S. Quick, J. Kaschke, C. Barner‐Kowollik, M. Wegener, Advanced Optical Materials 3(2) (2014) 221-232.
[115] C. Yuan, J. Liu, T. Jia, K. Zhou, H. Zhang, J. Pan, Z. Sun, Journal of Nonlinear Optical Physics & Materials 23 (2014) 02.
[116] Y. Cao, Z. Gan, B Jia, R. A. Evans, M. Gu, Optics express 19(20) (2011) 19486-19494.
[117] T. L. Andrew, H. Y. Tsai, R. Menon, Science 324(5929) (2009) 917-921.
[118] Z. Gan, Y. Cao, R. A. Evans, M. Gu, Nature communications 4 (2013).